Numerical Modelling of the Poiseuille Flow in the Microchannel Using the Boltzmann Equation

O. I. Rovenskaya

DiEM Dipartimento di Energetica e Macchine University of Udine, via. delle Scienze, 208, 33100 Udine, Italy

Abstract. The pressure-driven Poiseuille gas flow in two- dimensional microchannel with aspect ratio 10 is numerically investigated using the Boltzmann kinetic equation. The pressure ratio between the inlet and outlet of the channel is varied from 2.07 to 3.06 and the value of the exit Knudsen numbers Kn_e ranging between slip 0.027 and transitional 0.22 regimes. The validity of the first and second order slip boundary conditions is discussed. The comparison with the results calculated by means of the Navier - Stokes equations with slip boundary conditions shows that second order models are valid for Kn_e up to 0.22, whereas the first order one is accurate for $Kn_e \leq 0.055$.

Keywords: the Boltzmann equation; gas flow; microchannel; the discrete velocity method.

INTRODUCTION

In recent times, there has been increasing interest in computing flows with the more fundamental kinetic equations for applications involving atmospheric re-entry, hypersonic flight, astrophysical gas dynamics and flows in microscale devices [1]. In these applications the utility of the Navier – Stokes (NS) equations may be limited due to rarefied gas effects or lack of appropriate constitutive or state relations. NS models are generally valid if Knudsen number $Kn < 0.01$, but can be extended into the slip-flow regime ($0.01 < Kn < 0.1$) and partially to the transition flow regime $Kn < 0.25$ by appropriate treatment of the wall boundary [2-4]. In practice, gas flows in microchannels may encounter a wide range of conditions that include the continuum, slip and transition regimes. Therefore, the numerical modelling of microflows with the more fundamental Boltzmann kinetic equation is of great interest. It is expected that the application of the Boltzmann equation will give more general and correct results. The kinetic Boltzmann equation describes the evolution of a one-particle distribution function and enjoys validity over a wide range of transport phenomena than the continuum NS equation. In general, the Boltzmann equation is an integro-differential equation with a complicated nonlinear collision operator. Therefore, many investigators prefer to use different collision models to approximate the Boltzmann collision integral. In the present work the discrete velocity method [1, 5] for the approximation of the Boltzmann equation is applied. Direct solution of the Boltzmann equation methods can be much more accurate, and can be competitive with Monte-Carlo methods for problems in which the solution is not very far from thermodynamical equilibrium, and high accuracy is required. Moreover, in the most of the literature references the numerical solution of Boltzmann equation is used for investigation of external flows. Thus, it is interesting to apply this equation for the analysis of internal flows over a wide range of Kn.

STATEMENT OF THE PROBLEM AND NUMERICAL METHODS

In the present work the two dimensional problem of laminar flow in a rectangular microchannel, with height $H = 1$ μm and length $L = 10$ μm, is considered. To avoid difficulties in inlet and outlet boundary conditions, inlet and outlet zones of free flow with a length of $0.1L$ and $0.2L$, respectively, are introduced. The gas flows through channel due to a pressure difference between inlet and outlet. The inlet total pressure p_{0i} ranges from 2.07×10^5 to 3.06×10^5 Pa, while the outflow exit pressure p_e is kept constant at 10^5 Pa.

$$\frac{p_{0i}}{p_e} = \left(1 + \frac{\gamma - 1}{2} Ma_{is}^2\right)^{\gamma/(\gamma-1)}, \quad \frac{T_{0i}}{T_0} = \left(1 + \frac{\gamma - 1}{2} Ma_{is}^2\right).$$

Compressibility effect is monitored via the local value of Mach number *Ma* and the isentropic exit Ma_{is}, i.e. the *Ma* that would arise from an isentropic flow with the same pressure ratio as the real one. The wall temperature T_w is constant and equals to the inlet total temperature T_{0i}. In analogy to the Ma_{is}, an isoentropic Reynolds number Re_{is}, using the isoentropic exit mass flow, computed with the density ρ_{is} and velocity u_{is} for isoentropic flow, and an isoentropic Kn_{is} (for hard sphere model) are defined as

$$\mathrm{Re}_{is} = \frac{\rho_{is} u_{is} H}{\mu},\ u_{is} = Ma_{is} a,\ \frac{\mu}{\mu_0} = \sqrt{\frac{T}{T_0}},\ Kn_{is} = \frac{\lambda_{is}}{H} = \frac{16}{5}\frac{Ma_{is}\sqrt{\gamma/2\pi}}{\mathrm{Re}_{is}},$$

where $a_0 = \sqrt{\gamma R T_0}$ is a speed of sound, μ is viscosity, T_0, μ_0 are reference values, λ_{is} is a mean free path for an isoentropic state. Nitrogen is used as working gas; specific heat ratio is $\gamma = 1.4$, Prandtl number $\mathrm{Pr} = 0.72$. For the kinetic statement Kn_{is} is chosen from 0.025 (slip regime) to 0.2 (transitional regime). Continuum computations are carried out for the corresponding Re_{is}. Regular Reynolds, based on an actual computed mass flow, will be smaller.

Two different series of computations based on the kinetic approach were carried out. In the former, *Kn* is kept constant ($Kn_{is} = 0.0375$ and 0.1) over a range of pressure ratio (see Table 1), in the latter pressure ratio is kept constant and equals 2.07, while a range of Knudsen number (see Table 1) are considered.

TABLE 1. Isoentropic and exit conditions.

Ma_{is}	p_{0i}/p_e	Kn_e	Re_e
1.075	2.07	0.027÷0.22	22.78÷1
1.157	2.29	0.04, 0.11	14.45, 3.28
1.233	2.5	0.04, 0.11	16.8, 3.93
1.318	2.84	0.04, 0.11	19.93, 4.67
1.372	3.06	0.04, 0.11	22.18, 5.24

The numerical method is based on the direct numerical solution of the Boltzmann equation:

$$\frac{\partial f}{\partial t} + \xi \frac{\partial f}{\partial \mathbf{x}} = J(f,f) = \int_0^{2\pi}\int_0^{\sigma_{eff}} (f' f_*' - f f_*) g b db d\varepsilon d\xi_* = -\nu(f) f + N(f,f), \qquad (1)$$

where $\nu(f)f$ is the integral of "direct collisions", $\nu(f)$ is the frequency of collisions and $N(f,f)$ is the integral of "inverse collisions", $f = f(t,\mathbf{x},\xi)$ is the distribution function, ξ, ξ_*, ξ', ξ_*' are velocities of pair of particles before and after collision, $J(f,f)$ is the collision integral, $\mathbf{g} = \xi_* - \xi$ is the relative velocity, and b, ε are impact parameters. In the rest of the paper the non-dimensional formulation of the problem is used, the scale quantities are the follows: $v_0 = \sqrt{2RT_0}$ is the thermal velocity, H is height of the channel, effective radius σ_{eff} equals to the radius σ_∞ of hard-sphere particles, n_0 and T_0 are characteristic density and temperature respectively.

For the discretization of (1), the 3D Cartesian grid $\{\xi_\gamma\}$ with equidistant nodes is defined in the velocity space, and the grid $\{x_i, y_j\}$ is defined in the physical space. Introducing of the grid values the obtained set of equations for $f_{\gamma ij}$ can be numerically solved using time splitting method. In a small time interval Δt, the numerical solution of the transport step (2) and the space homogeneous collision step (3) are considered. The transport part is approximated by a standard finite volume scheme:

$$f_{\gamma,i,j}^{*n+1} = f_{\gamma,i,j}^{*n} - \frac{\Delta t}{\Delta x}\left(F_{\gamma,i+1/2,j}^{n} - F_{\gamma,i-1/2,j}^{n}\right) - \frac{\Delta t}{\Delta y}\left(F_{\gamma,i,j+1/2}^{n} - F_{\gamma,i,j-1/2}^{n}\right),\ f_{\gamma,i,j}^{*n} = f_{\gamma,i,j}^{n} \qquad (2)$$

$$F_{\gamma,i+1/2,j}^{n} = \frac{1}{2}\left(\xi_x^\gamma\left(f_{\gamma,i+1,j}^{*n} + f_{\gamma,i,j}^{*n}\right) - \left|\xi_x^\gamma\right|\left(\Delta f_{\gamma,i+1/2,j}^{n} - \Phi_{\gamma,i+1/2,j}^{n}\right)\right),\ \Delta f_{\gamma,i+1/2,j}^{n} = f_{\gamma,i+1,j}^{*n} - f_{\gamma,i,j}^{*n},$$

where $F_{\gamma,i+1/2,j}^{n}$ is the numerical fluxes, and $\Phi_{\gamma,i+1/2,j}^{n} = \min\mathrm{mod}\left(\Delta f_{\gamma,i-1/2,j}^{n}, \Delta f_{\gamma,i+1/2,j}^{n}, \Delta f_{\gamma,i+3/2,j}^{n}\right)$ is the flux limiter function, provided a second order of the scheme. The time step follows the condition:

$\Delta t = CFL / \max\left(V_{\max}/\Delta x + V_{\max}/\Delta y\right)$, where CFL is the Courant number, $V_{\max} = 4\sqrt{T_{0i}}$ is a boundary of the velocity space and Δx and Δy are the mesh sizes in the x and y directions, respectively. To approximate collision step the explicit-implicit approach is applied.

$$\frac{f_{\gamma,i,j}^{n+1} - f_{\gamma,i,j}^{n}}{\Delta t} = \frac{1}{Kn\sqrt{2}\pi}\left(-\nu(f_{\gamma,i,j}^{n}) f_{\gamma,i,j}^{n+1} + N(f_{\gamma,i,j}^{n}, f_{\gamma,i,j}^{n})\right),\ f_{\gamma,i,j}^{n} = f_{\gamma,i,j}^{*n+1}. \tag{3}$$

where the frequency of collisions $\nu(f)$ and the "inverse collisions" integral $N(f,f)$ are taken from the time level n and the velocity distribution function from $n+1$ level. The quasi - Monte-Carlo method, in which Korobov sequences are used [5], is employed for calculation of the $\nu(f)$ and $N(f,f)$. In the general case, the post-collision velocities do not coincide with grid nodes in the velocity space. Therefore, to ensure the execution of conservative laws the procedure of redistribution energy between nearest nodes in velocity grids (for each collision) is used [5]. This approach provides with microscopic (kinetic) conservation for each collision. Since in the explicit-implicit method the distribution function is taken from the upper time level the procedure of conservative correction should be applied [1]. The conservative correction procedure ensures the positive value of the distribution function after relaxation stage. Therefore, velocity distribution function has acceptable accuracy even if coarse grid is used.

Maxwell diffuse reflecting boundary conditions with the full accommodation on channel walls are applied. For all particles coming off the surface it is assumed that molecules are emitted with the Maxwell distribution functions corresponding the zero mean flow velocity, the temperature is equal to the wall temperature T_w and the density calculated from the condition of equality of the fluxes of particles coming on and off the wall. At the central line of the channel the specular boundary condition is imposed.

Flow quantities at inlet and outlet boundary faces are determined using the theory of the characteristics in accord with standard CFD practices, assuming adiabatic and isentropic flow conditions [6, 7]. The Maxwell velocity distribution function is assumed for molecules entering from the inlet and outlet boundaries into the solution domain. At the inflow boundary, the pressure p_{0i}, temperature T_{0i}, and transverse velocity v_i are generally specified, where the transverse velocity is assumed to be zero and only the streamwise velocity should be calculated. The inlet zone is 10% of the wall length and is considered as a specular reflector. This consideration would provide more realistic condition at the channel inlet in microflow treatments [7]. At the outflow variables except pressure are determined from the simulation. According to the theory of characteristic the exit pressure directly influences the velocity of the molecules adjacent to the outlet boundary and the thermodynamic properties of the cells located near the outlet, allowing for an exit pressure in the channel larger then the actual back pressure, in the case of choked flow. Hence, a nonphysical prediction of the flow field in the Boltzmann equation statement [7] may be obtained. To properly implement the physics of flow, the back pressure is applied right at the outer region of the buffer zone, considered as a free flow one. Therefore, the solution is permitted to freely adjust at the real outlet. Influence of size of buffer zone on the flow has been carried out and computations were made for buffer zone equals 20% of the wall length L.

A second order scheme can be easily derived simply by symmetrizing the first order scheme: transport step over the time interval $\Delta t/2$, relaxation one over the time interval Δt, and again transport one over $\Delta t/2$, provided every step is solved with a method at least second order accurate in time.

Parallelization in physical space is made to improve the efficiency of the algorithm. Each processor is assigned its own set of points in physical space to compute the distribution function at these points. The relaxation stage is calculated independently on the various processors. Before the stage of transport, the processors exchange data at neighboring points not assigned to this processor. The software code was written in C++ with the use of MPI (Message Passing Interface).

RESULTS AND DISCUSSION

To compare with continuum results the viscous, compressible NS equations for 2D laminar flow are solved by employing a hybrid finite difference-finite volume method. For the time integration implicit, spatially factored ADI scheme proposed by Beam and Warming is used. The program in FORTRAN has been developed by Croce et. al. for the simulations of microflows [8]. Here, a range of Kn_e between 0.027 (slip regime) and 0.22 (transition regime) is considered, where the continuum NS equations may be used, provided that slip flow condition is enforced at the wall. At lower values of Kn, up to 0.1, it is expected that the Maxwell first order slip flow condition is adequate [3, 4], for larger Kn second order slip boundary conditions (as suggested by Cercignani [9] and Diessler [10]) are applied and the Smoluchowski temperature jump boundary conditions:

$$u_{y=0} - u_w = \alpha \left[A_{v1} \lambda \frac{\partial u}{\partial y} - A_{v2} \lambda^2 \frac{\partial^2 u}{\partial y^2} \right]_{y=0}, \quad T_{y=0} - T_w = \beta \left[A_{T1} \lambda \frac{\partial T}{\partial y} - A_{T2} \lambda^2 \frac{\partial^2 u}{\partial y^2} \right]_{y=0},$$

where $\alpha = \beta \approx 1.1$ for a hard sphere gas [11, 12] and coefficients A_{v1}, A_{v2}, A_{T1} and A_{T2} are presented in Table 2.

TABLE 2. Values of slip coefficients proposed in the literature.

Source	A_{v1}	A_{v2}	A_{T1}	A_{T2}
Maxwell	1	0	1.62	0
Diessler	1	1.125	1.62	3.011
Cercignani	1.1466	0.9756	1.62	-0.81

The numerical method and treatment for the inflow and outflow boundaries for the Boltzamnn equation has been validated by comparison with results of Nance et al. [6], obtained by DSMC method, for a short microchannel with length of 5 μm and height of 1 μm and 30 × 84 nonuniform grid. The inlet temperature T_{0i} is 300 K and equals T_w. Constant pressure ratio $p_{0i}/p_e = 3.18$ ($Ma_{is} = 1.33$) is assumed with $Kn_e \approx 0.05$ ($Kn_{is} = 0.04$). The results for centerline streamwise velocity, static pressure and density from NS and Boltzmann solutions are presented in Fig. 1 (*a*, *b*, *c*). The kinetic results show satisfactory agreement with those of Nance [6], except the inlet region for streamwise velocities where the difference is larger. As expected, a comparison with continuum quantities demonstrates more noticeable discrepancies.

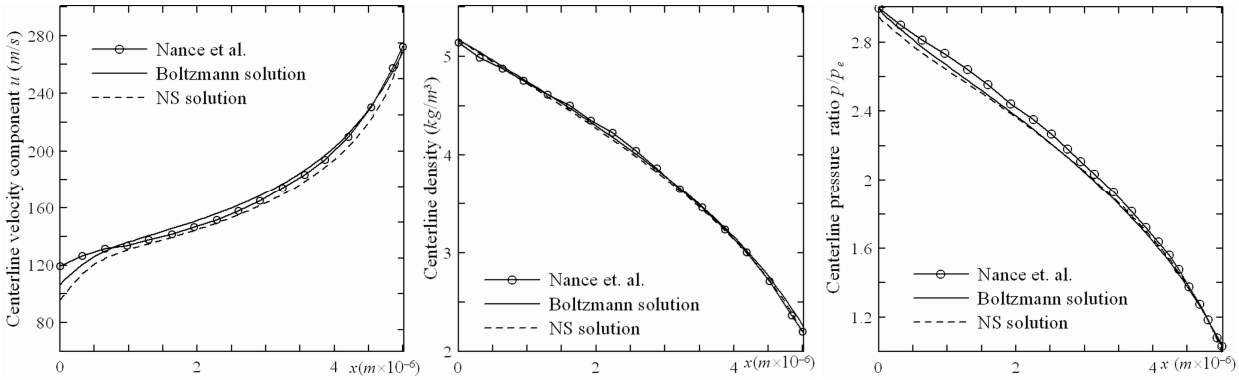

(*a*) (*b*) (*c*)

FIGURE 1. Centerline velocity, density and pressure along channel for the kinetic and continuum approaches and $Kn_e = 0.05$.

In simulation, the geometrical symmetry allows for the discretization of just one half of the channel. A nonuniform structured grid 112 × 30 for the kinetic statement and 144 × 24 mesh for the continuum one are used. Grid independence tests have been carried out in order to assess the accuracy of the mesh. The velocity space is bounded by $V_{\max}$: $-V_{\max} \le \xi \le V_{\max}$ and the step is $\Delta\xi = 0.37$. The decrease of $\Delta\xi$ did not have a large effect on the flow pattern (error of 1%). The time step is restricted by $CFL = 0.8$ and the dimensionless time step Δt varies from 2.5×10^{-3} to 3.5×10^{-3}. The solution is considered as converged when the variation of the mass flow rate between entrance and exit regions is less then 1 %. The calculations were conducted using multicores system consisted of 2 processors with 4 cores. The CPU time was about 360 h for fully developed flow (nondimensional time equals 80).

The pressure ratio p_{0i}/p_e varied from 2.07 to 3.06 (see Table 1) for fixed $Kn_e = 0.04$ and 0.11 are considered. Fig. 2 (*a*, *b*) shows the averaged over cross section pressure and the Mach number distributions along the channel for the different inlet pressures and the constant $Kn_e = 0.04$ compared with results based on the NS equations with the first order slip boundary conditions and without (no-slip solution). As expected, for this Kn_e results obtained by the Boltzmann equation are close to ones of NS equation coupled with the first order slip boundary condition and deviate significantly from results of no-slip NS solution. The mass flow rate distribution demonstrates the same behavior (see Fig. 3 *a*). The magnitudes of the mass flow rate of the Boltzmann equation are close to ones of NS equations with the first order boundary conditions, while the solution of NS equations with no-slip boundary condition is quite different from both. For larger $Kn_e = 0.11$ second order boundary conditions for NS equations are applied. In Fig. 2 *c* averaged *Ma* and pressure distribution are compared with solutions of NS equations with the first order and second order Cercignani and Diessler boundary conditions. There is a clear difference between *Ma* distributions obtained from the solution of the kinetic equation and NS ones. Nevertheless, the difference in pressure

distributions is much less evident (see Fig. 2 *d*) since the compressibility effect, responsible for the curvature of the pressure profile, is of the same order of magnitude (as is the Mach number).

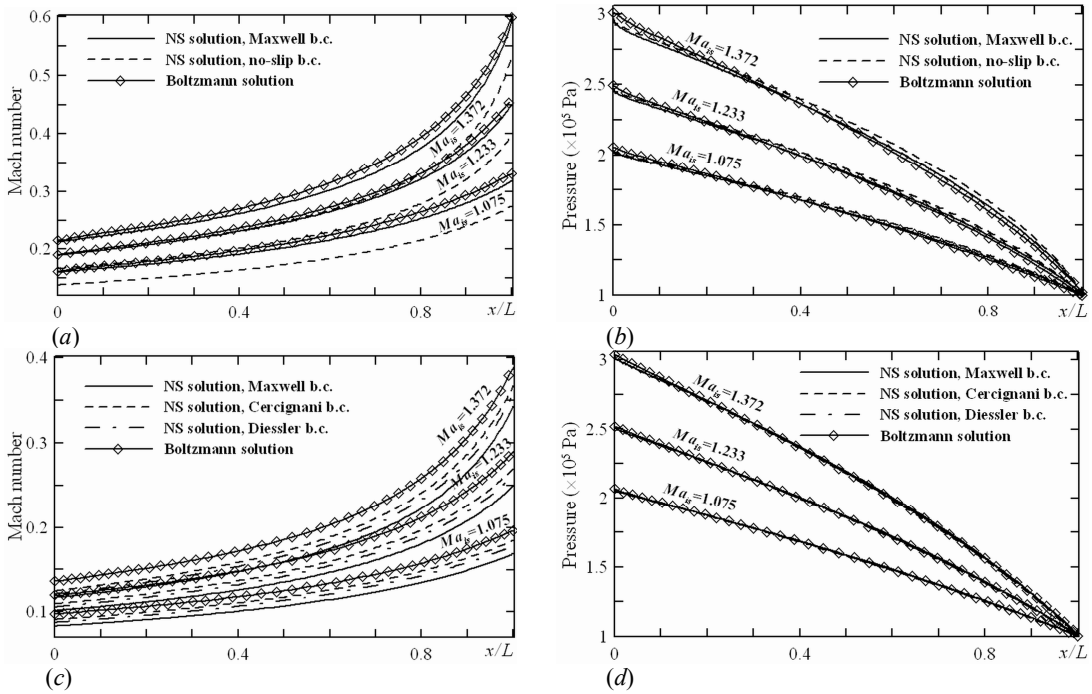

FIGURE 2. Averaged Mach number and pressure distributions along the channel for the kinetic and continuum approaches, different inlet pressures and $Kn_e = 0.04$ (*a*, *b*), 0.11 (*c*, *d*).

The mass flow rates for different pressure ratios obtained by both approaches are shown in Fig. 3 *b*. For larger $Kn_e = 0.11$ the difference between results computed by the Boltzmann equation and ones of NS equations with the Maxwell boundary condition becomes larger, approximately 15 %. Solutions with second order boundary conditions are closer to the kinetic one. The maximal deviation from the kinetic solution appears for large pressure ratio and is 9% for Diessler boundary condition and 5.6 % for Cercignani one.

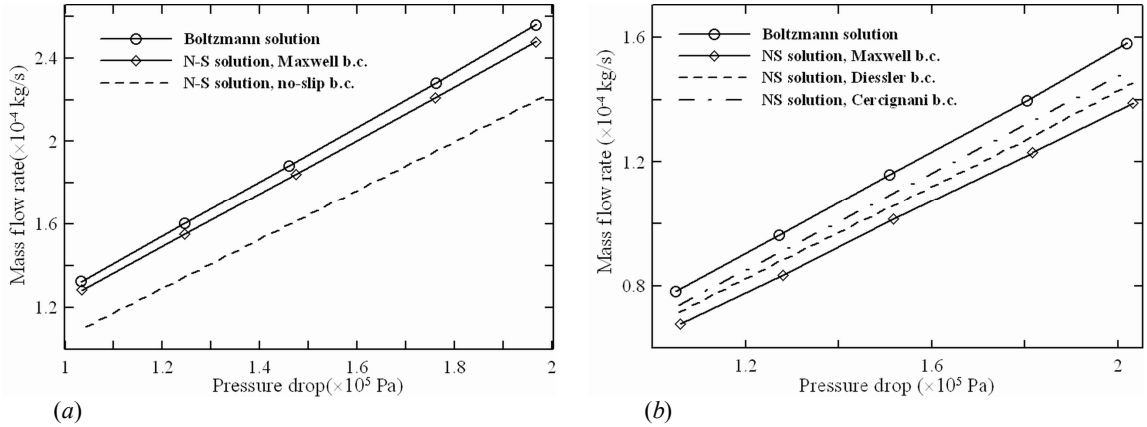

FIGURE 3. Mass flow rates for the kinetic and continuum approaches, different pressure drops and $Kn_e = 0.04$ (*a*), 0.11 (*b*).

The influence of rarefaction on gas flow is investigated. The computation is carried out for constant pressure deference 2.07 and the exit Knudsen number ranging from 0.027 (slip regime) to 0.22 (transition regime). Comparisons between averaged Mach number distribution of the Boltzmann solution and NS ones with first and second order boundary conditions are presented in Fig. 4 *a*. Results obtained by NS equations with first order boundary conditions agree well with Boltzmann ones until $Kn_e < 0.11$. The use of second order boundary conditions

gives distributions of averaged *Ma* well corresponding to the kinetic ones for all range of Knudsen. A comparison of the mass flow rates with the results based on the NS equation with the first and second order slip boundary conditions are shown in Fig. 4 *b*. For $Kn_e < 0.11$ the mass flow rate predicted by the Boltzmann equation is close to the predicted by the NS equations for both first and second boundary conditions, at least for any engineering purpose (for first order model the difference is negligible up to 0.055). For $Kn_e \geq 0.11$ the difference becomes remarkable and growth with *Kn*. Although always underestimated the mass flow rates obtained by NS equations with second order either Cercignani or Diessler boundary conditions remain close to the Boltzmann solution even for $Kn_e = 0.22$. The obtained ranges of Kn_e in which slip boundary conditions models are valid agree well with those pointed out in [2].

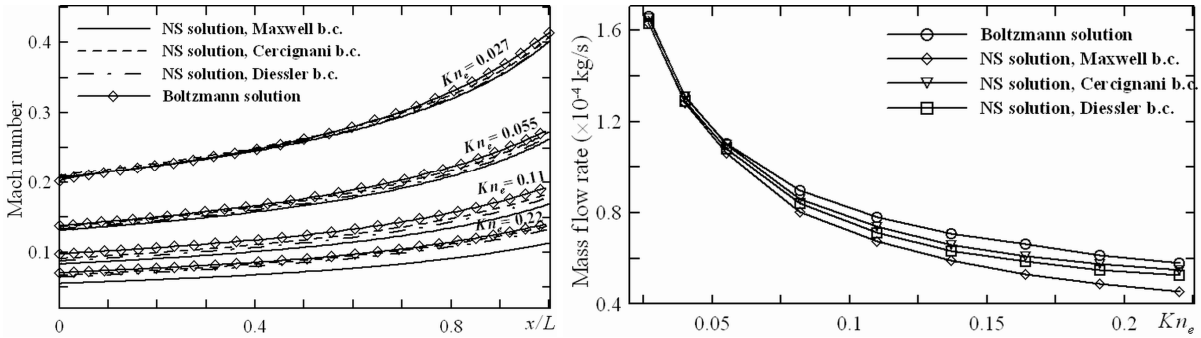

FIGURE 4. (*a*) Averaged Mach number distributions along the channel for $Kn_e = 0.027$, 0.055, 0.11 and 0.22; (*b*) Mass flow rates via Kn_e compared with results based on NS equations with the first and second boundary conditions.

CONCLUSIONS

The numerical investigation of gas flow in microchannel based on the direct numerical solution of Boltzmann equation has been carried out. The numerical method and treatment for the inflow and the outflow boundary conditions have been successfully validated by comparison with DSMC method [6]. The comparison with the solution of the Navier-Stokes equations shows that the differences between those approaches are negligible up to $Kn_e \leq 0.055$. Significant discrepancies appear and grow in transitional regime. However, while the first order boundary condition seems inadequate above $Kn_e = 0.11$, the use of second order boundary conditions offers reasonable engineering accuracy up to the transition regime, until $Kn_e \leq 0.22$. Kinetic results, however, always predict higher mass flow rate.

ACKNOWLEDGMENTS

The author is thankful to V.V. Aristov and G. Croce for helpful discussions and advices.

The research leading to these results has received funding from the European Community's Seventh Framework Programme (ITN - FP7/2007-2013) under grant agreement n° 215504.

REFERENCES

1. V.V. Aristov, *Methods of Direct Solving the Boltzmann Equation and Study of Nonequilibrium Flows*, New York: Springer, 2001, p. 324
2. S. Colin, P. Lalonde, and R. Caen, *Heat Transfer Engineering* **25**, 23 - 30 (2004).
3. E.B. Arkilic, M.A. Schmidt, and K.S. Breuer, *J. Microelectromech. Syst.* **6**, 167–178 (1997).
4. M. Gad-el-Hak, *J. Fluids Engineering* **121**, 5-33 (1999).
5. F. Tcheremissine, "Direct Numerical Solution Of The Boltzmann Equation " in *24th Symposium on Rarefied Gas Dynamics*, edited by M. Capitelli, AIP Conference Proceedings 762, American Institute of Physics, Melville, NY, 2005, pp. 677-685.
6. R.P. Nance, D.B. Hash and H.A. Hassan, *J. Thermophysics and Heat Transfer* **12**, 447 - 449 (1998).
7. E. Roohi, M. Darbandi and V. Mirjalili, *J. Heat Transfer* **131**, 1-8 (2009).
8. G. Croce, P. D'Agaro and A. Filippo, *Heat Transfer Eng.* **28**, 688 – 695 (2007).
9. C. Cercignani, A. Daneri, *J. Appl. Phys.* **34**, 3509 – 3513 (1963).
10. R.G. Deissler, *Int. J. Heat Mass Transfer* **7**, 681–694 (1964).
11. D.L. Morris, L. Hannon and A.L. Garcia, *Phys. Rev. A* **46**, 5279–5281 (1992).
12. S. K. Loyalka, *Phys. Fluids* **1**, 403 – 408 (1989).